

RESEARCH PAPER

Cerium oxide nanoparticles mitigate retinal pigment epithelium (RPE) death using APRE19 cell model

Eric Dahl ^{1*}, Nikolaos E Efstathiou ², Amit K. Roy ³

¹New York Institute of Technology College of Medicine, Old Westbury, NY, USA

²Massachusetts Eye & Ear Infirmary, Boston, MA, USA

³Department of Chemical Engineering, Northeastern University, Boston, MA, USA

ABSTRACT

Objective(s): In this study, we present the potential of cerium oxide nanoparticle pretreatment on ARPE-19 cells, a cell line of the Retinal Pigment Epithelium (RPE), as a therapeutic modality to cellular stresses such as low serum starvation.

Materials and Methods: ARPE-19 cells were pretreated with nano-cerium oxide at a concentration of 500 µg/mL before low serum stress was induced for 24, 48, 72, and 96 hours. Starvation stress was induced by using low concentrations of Fetal Bovine Serum (FBS) media at three increments: 10%, 1%, 0.1%.

Results: Contrast images demonstrated higher cell confluence and cell integrity in cells pretreated with cerium oxide nanoparticles compared to untreated cells. Increased cell viability for cerium oxide pretreated cells was confirmed by MTS assay after 96 hours of serum starvation.

Conclusion: By using nanoparticles to influence pathways of apoptosis, we hope to rescue ARPE-19 cells from a range of stressors, including oxidative stress, and re-establish homeostasis for the cell. Nanoparticles may represent a novel class of therapeutics for diseases of the eye, like AMD and blue-light induced oxidative stress.

Keywords: Blue light, Cerium oxide, Macular degeneration

How to cite this article

Dahl E, Efstathiou N, K. Roy M. Cerium oxide nanoparticles mitigate retinal pigment epithelium (RPE) death using APRE19 cell model. *Nanomed J.* 2021; 8(1): 14-20. DOI: 10.22038/nmj.2021.08.02

INTRODUCTION

Age-related macular degeneration (AMD) is the most common cause of vision loss in the elderly in the Western world [1]. AMD consists of a group of clinically distinct diseases that affect the central retina, resulting in a range of symptoms. The severity of these symptoms can progress from subtle distortions to reduced visual acuity in the perception of fine details to an eventual complete loss of central vision and/or legal blindness. AMD is characterized initially by a progressive, slow degenerative loss of the retinal pigment epithelium (RPE). The RPE is essential for photoreceptor cell renewal and maintenance of the blood-retina barrier and plays a role in the visual cycle. Thus, AMD causes progressive loss and degeneration of both photoreceptor cells above the RPE and the choriocapillaris below them. The

precise mechanisms of RPE loss are unknown [2]; however, multiple lines of evidence point towards cumulative oxidative damage as a causal role in RPE cell death [3]. The RPE is continually exposed to a high concentration of oxygen in the macular region, abundance of reactive oxygen species (ROS), and intensive light irradiation [4-6]. With time, these adverse factors on RPE cells contribute to the overall reduction in antioxidant capacity seen with age and increase the levels of lipid- and protein-based pro-oxidative products [2, 7].

Epidemiological studies have identified a variety of risk factors for AMD; with smoking as the leading environmental factor [8]. Cigarette smoke contains over 4000 different substances, many of which are potent oxidants including hydroquinone (HQ) [9-11]. Chronic oxidative damage can upset the balance of the antioxidant response, leading to irreparable macromolecular damage that triggers cell death. The oxidative effects of

* Corresponding Author Email: dahl.e@northeastern.edu

Note. This manuscript was submitted on July 26, 2020; approved on October 19, 2020

cigarette smoke on the eye have been well studied and are known to generate drusen-like deposits, promote choroidal neovascularization, exert mitogenic effects on many cell types, and cause RPE transcriptome alterations affecting autophagy, immune responses, mitochondrial function and survival [12-14].

Another stressor known to increase oxidative damage includes short wavelength light, or blue light. Blue light was shown to result in a decrease of a-waves and b-waves in an illuminance-dependent manner, which characterizes an impaired electrical response to light in the eye [15, 16]. Blue light will penetrate the lens of the eye to cause retinal photochemical damage and massive apoptosis, leading to damage of the RPE [17, 18]. RPE damage causes photoreceptor death and ultimately progressive blindness will ensue, similarly to the pathogenesis of AMD.

In this study, we present the potential of cerium oxide nanoparticle pretreatment on ARPE-19 cells, a cell line of the RPE [19], as another therapeutic modality to cellular stresses such as oxidative damage, exposure to blue light, and low serum stress. Pretreatment with cerium oxide nanoparticles can provide a non-toxic way to penetrate ARPE-19 cells and provide cytoprotective effect, reducing damage to the RPE.

Specifically, we tested the viability of ARPE-19 cells when pretreated with cerium oxide nanoparticles at a concentration of 500 µg/mL under starvation stress conditions. Starvation stress was induced using low concentrations of Fetal Bovine Serum (FBS) media at three increments: 10%, 1%, 0.1%. Contrast images were taken at 24, 48, 72, and 96 hours. MTS assay was conducted at 96 hours.

MATERIALS AND METHODS

Cerium Oxide Nanoparticle Preparation & Sizing

The chemicals used in this experiment were acquired from Sigma (St. Louis MO, USA), and utilized without additional purification. Cerium oxide nanoparticles were synthesized by mixing a cerium nitrate hexahydrate solution with a sodium hydroxide solution. The mixture was then left to dry for 24 hours [20].

The cerium nitrate hexahydrate solution was prepared by mixing 21.7 g of cerium nitrate hexahydrate with 100 mL of water. The sodium hydroxide solution was prepared by adding 2 g of sodium hydroxide to 50 mL of distilled water.

To form the cerium oxide nanoparticles, 85 mL of ceria nitrate solution, 5 mL of sodium hydroxide solution, and 75 mL of distilled water were added to a beaker. The solution was stirred for 1 hour and then left at 150°C for 24 hours.

Cerium oxide nanoparticles were assessed for size using transmission electron microscopy (TEM). The cerium oxide nanoparticles were suspended in ethanol, then placed in a carbon grid for analysis. A JEOL JEM-101 TEM was used to determine the average size and distribution of Ce NPs.

Cell culture

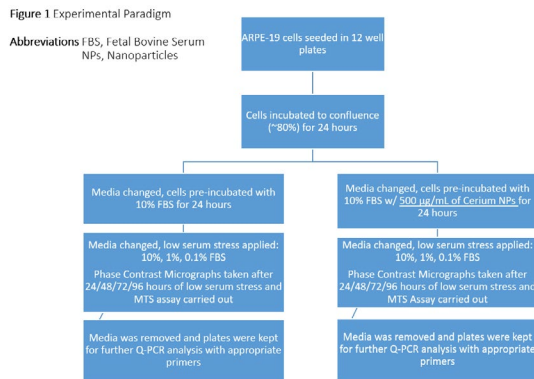
ARPE-19 cells were cultured in Dulbecco's Modified Eagle's Medium (DMEM) with high glucose and L-glutamine. Cell culture also contained 10% heat-inactivated Fetal Bovine Serum (FBS), 100 U/mL penicillin G, 100 mg/mL streptomycin, 250 µg/mL amphotericin B. The ARPE-19 cell cultures were grown to confluency in 100mm plates. The cell cultures were maintained in a humidified chamber at 37 °C with 5% CO₂ and 95% air atmosphere. Culture medium was changed every 48 hours. ARPE-19 cells used for the experiments in this study were of passages 3-4. After confluency of ARPE-19 cells were reached (80-90% confluence), the cells were detached from 100mm plates with 500 µL of TripleE to create a suspension. The suspension was centrifuged in 15 mL screw cap tubes, and then reconstituted in DMEM complete medium, with FBS and other supplements listed above. Cells were visualized under a light microscope for morphology.

Serum starvation

Before serum starvation was applied, ARPE-19 cells were transferred from their original culture plates to new plates. ARPE-19 cells were seeded at a concentration of 40,000 cells/well on twelve well plates for 24 hours to ~80% confluence. Complete media contained DMEM with high glucose and L-glutamine, with 10% heat inactivated FBS, 100 U/ml penicillin G, 100 mg/mL streptomycin, 250 µg/mL amphotericin B. Pretreatment of ARPE-19 cells with nanoparticles involved replacing old medium with complete medium containing 500 µg/mL cerium oxide nanoparticles. Pretreated ARPE-19 cells were incubated for 24 hours.

To apply serum starvation, low serum medium was added at concentrations of 1% FBS and 0.1% FBS to their respective wells, along with the same DMEM, 100 U/mL penicillin G, 100

mg/ml streptomycin, 250 µg/mL amphotericin B as described in the cell culture section. Plates containing 10%, 1%, and 0.1% media were incubated in a humidified chamber at 37 °C with 5% CO₂ and 95% air atmosphere for 24, 48, 72, and 96 hours. Fig 1 is a visualization of the experimental paradigm used in this experiment.



Fi 1. Experimental Paradigm

Abbreviations: FBS, fetal bovine serum; NPs, nanoparticles

Contrast images

Phase contrast images of the twelve well plates containing ARPE-19 cells were acquired at 0, 24, 48, 72, and 96 hours at each concentration of FBS stress. A Nikon Eclipse TS100 microscope was used to image the cell plates. Each well was imaged two times in central areas of the well to minimize edge effects. Every image taken was evaluated for confluence and morphology. One image per sample was included in the results section.

Cell viability MTS assay

ARPE-19 cells were seeded at 5000 cells per well and grown to confluence for 24 hours. Pretreatment of cerium oxide nanoparticles was applied to ARPE-19 cells and then incubated for an additional 24 hours. Low serum stress was applied at 10%, 1%, 0.1% concentrations of FBS. MTS Cell Proliferation Assay was conducted after 96 hours of low serum stress. To determine the percent viability of cells pretreated with cerium oxide nanoparticles, the data was normalized to untreated ARPE-19 cells at FBS concentration of 10%.

Statistical analysis

Each experiment presented in this paper was conducted three times. With data collected from the MTS assay, a two-sample t-test of unequal

variances was conducted to compare the effect of cerium oxide nanoparticles with untreated cells for each FBS concentration.

RESULTS

Synthesized cerium nanoparticles were characterized with transmission electron microscopy (TEM) before preincubation with ARPE-19 cells. Fig 2 shows a TEM image of cerium nanoparticles with four different observable diameters, ranging from 8.34 nm to 10.2 nm.

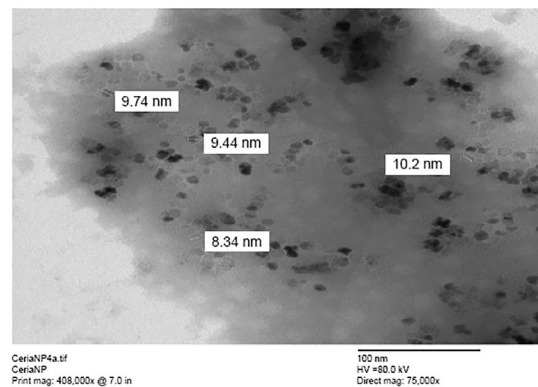


Fig 2. Cerium nanoparticles characterized with transmission electron microscopy

Abbreviations: NPs, nanoparticles; Mag, magnification

Phase contrast micrographs of ARPE-19 cells were obtained 0, 24, 48, 72, 96 hours after applying serum starvation. For all periods of low serum starvation, 10% FBS concentration without nanoparticles served as the control.

We first identified slight differences in ARPE-19 cell populations after 24 hours, as depicted in Fig 3. The top row represents cells that were left untreated, while the bottom row was preincubated for 24 hours with cerium oxide nanoparticles at a concentration of 500 µg/mL. Each column represents a different level of low serum stress, with 10% FBS serving as the control, 1% FBS as moderate stress, and 0.1% FBS as extreme stress. The stress effects on ARPE-19 cell populations were more apparent in Fig 4, which was taken after 48 hours of serum starvation.

In Fig 5 and Fig 6, acquired after 72 hours and 96 hours respectively, significant differences between treated and untreated ARPE-19 cell populations can be observed. Specifically, with 0.1% concentration of FBS at 96 hours, treated cells were highly confluent while untreated cells were sparse.

After 96 hours of low serum stress, an MTS assay was conducted to evaluate the percent viability of ARPE-19 cells pretreated with 500 µg/mL cerium oxide nanoparticles, when compared to untreated ARPE-19 cells. All three concentrations of FBS used for serum stress were analyzed in the MTS assay. Fig 7 presents quantitative results of the MTS assay. As noted on Fig 7, t-test for FBS concentration of 10% did not reveal a significant difference for cell viability when comparing presence of cerium oxide nanoparticles against absence of cerium oxide nanoparticles. T-tests conducted for FBS concentrations of both 1% and 0.1% indicated a statistically significant difference between presences of cerium oxide nanoparticles against absence of cerium oxide nanoparticles.

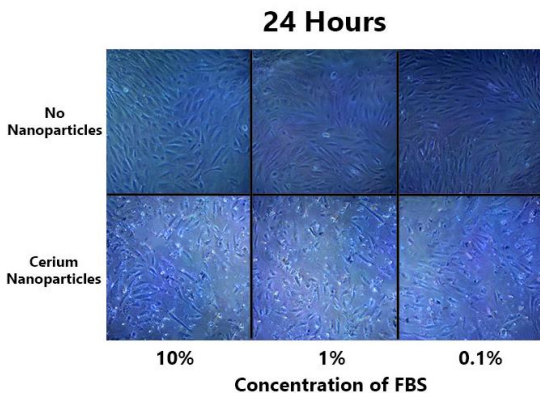


Fig 3. Nanoparticle treated ARPE-19 cells stressed by serum starvation after 24 hours

Notes: ARPE-19 cells were serum starved for 24 hours at varying concentrations (10%, 1%, 0.1%) of FBS, as indicated. The top row shows untreated ARPE-19 cells. The bottom row shows ARPE-19 cells pretreated with 500 µg/mL cerium oxide nanoparticles. Each column signifies a different level of FBS low serum stress. Magnification: 100x.

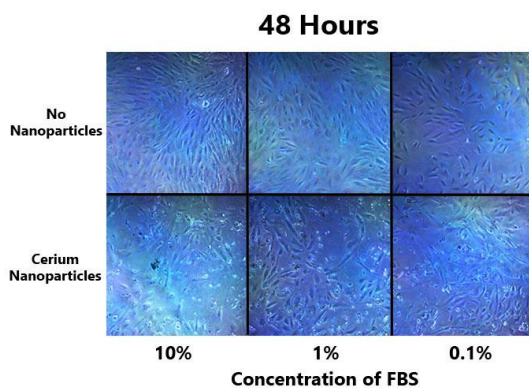


Fig 4. Nanoparticle treated ARPE-19 cells stressed by serum starvation after 48 hours

Notes: ARPE-19 cells were serum starved for 48 hours at varying concentrations (10%, 1%, 0.1%) of FBS, as indicated. The top row shows untreated ARPE-19 cells. The bottom row shows ARPE-19 cells pretreated with 500 µg/mL cerium oxide nanoparticles. Each column signifies a different level of FBS low serum stress. Magnification: 100x.

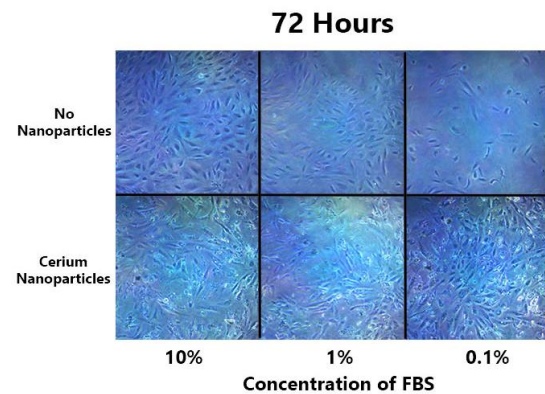


Fig 5. Nanoparticle treated ARPE-19 cells stressed by serum starvation after 72 hours

Notes: ARPE-19 cells were serum starved for 72 hours at varying concentrations (10%, 1%, 0.1%) of FBS, as indicated. The top row shows untreated ARPE-19 cells. The bottom row shows ARPE-19 cells pretreated with 500 µg/mL cerium oxide nanoparticles. Each column signifies a different level of FBS low serum stress. Magnification: 100x.

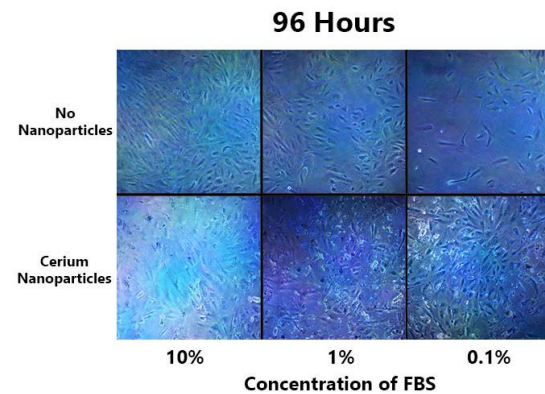


Fig 6. Nanoparticle treated ARPE-19 cells stressed by serum starvation after 96 hours

Notes: ARPE-19 cells were serum starved for 96 hours at varying concentrations (10%, 1%, 0.1%) of FBS, as indicated. The top row shows untreated ARPE-19 cells. The bottom row shows ARPE-19 cells pretreated with 500 µg/mL cerium oxide nanoparticles. Each column signifies a different level of FBS low serum stress. Magnification: 100x.

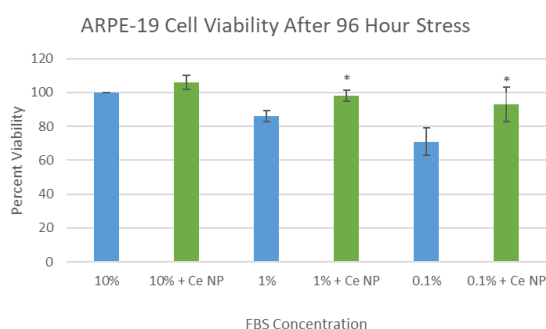


Fig 7. MTS Assay of ARPE-19 cells under 96 hours low serum stress

Notes: ARPE-19 cells were serum starved for 96 hours at varying concentrations (10%, 1%, 0.1%) of FBS, as indicated. Blue bars show results of ARPE-19 cells that were left untreated with cerium oxide nanoparticles. Green bars (+ Ce NP) show results of ARPE-19 cells that were pretreated with cerium oxide nanoparticles at a concentration of 500 µg/mL. Data was normalized to present the control, 10% FBS untreated with cerium oxide nanoparticles, as 100% ARPE-19 cell viability. *P<0.05 compared to the respective control, which was untreated with cerium oxide nanoparticles at the same FBS concentration.

DISCUSSION

As shown in our low serum experiments, ARPE-19 cells pretreated with cerium oxide nanoparticles at a concentration of 500 µg/mL 24 hours prior to starvation stress showed higher confluence, compared to control. This effect is first evident after 48 hours of low serum stress, as seen in Fig 4. Confluence differences for 72 and 96 hours of serum stress were even more apparent, as seen in Fig 5 and Fig 6 respectively. At these time markers, obvious sparsity of untreated ARPE-19 cells can be observed with 0.1% concentration of FBS. However, similar sparsity is not evident in ARPE-19 cells pretreated with 500 µg/mL cerium oxide nanoparticles when stressed at the same concentration of 0.1% FBS. These results suggest that the pretreatment of cerium oxide nanoparticles enabled cell rescue for stressed ARPE-19 cells.

MTS analysis conducted at 96 hours after low serum stress provides quantitative data to support the results obtained from phase contrast micrographs. As Fig 7 shows, nanoparticle-treated cells had a significantly higher cell viability for FBS concentrations of 1% and 0.1%. At 1% FBS

concentration, pretreatment with cerium oxide nanoparticles resulted in a 14% higher cell viability compared to untreated control. At 0.1% FBS concentration, the nanoparticle-induced rescue effect was even more pronounced, with a 22% higher cell viability in pretreated cells. Statistical analysis supports these findings as significant. The control wells, at 10% FBS concentration, had a relatively small 6% difference between untreated and pretreated cells. The data collected from 10% FBS wells were not found to be statistically significant. The cellular stress experiments at FBS concentrations 1% and 0.1% remain clear examples of nanoparticle-mediated cell rescue.

Within the human body, mechanisms of apoptosis are often induced with introduction of cellular stress such as hypoxia, extreme temperatures, or starvation conditions. The findings gathered from this study, involving low serum starvation conditions, may have implications on all types of stress experienced at the cellular level. Oxidative stress, for example, can be caused by cigarette smoke or photochemical reactions induced by blue light. These pathogenic factors cause intracellular misfolding of proteins, ultimately leading to apoptosis of the cells within the RPE and progressive blindness [14]. The ARPE-19 cell line is a part of the RPE, critical for maintenance and nutrition of photoreceptors that allow for vision. Protections from stress induced death of ARPE-19 cells, as shown in this study, provide insight on possible novel treatment routes for diseases that involve death of the RPE.

The mechanism of apoptosis in serum starved cells is likely to be similar as with oxidative stress. A well-studied mechanism of apoptosis is the Bcl-2 pathway. Bcl-2 activation will cause a cascade of actions within the mitochondria, including release of cytochrome c and the activation of caspases like caspase-9, which have been coined as the cell death executioners [21]. We believe the inhibition of the Bcl-2 pathway to be one mechanism of nanoparticle pretreatment, which allows ARPE-19 cells to live on in times of cellular stress.

Future studies must be conducted to investigate specific mechanisms of nanoparticle-related protection from cell death. As our next step in understanding the potential therapeutic benefit of nanoparticles, we would like to investigate the mechanism of nanoparticle-mediated cell rescue. Specifically, we suspect nanoparticles to inhibit the Bcl-2 apoptosis pathway, which we would like to

further research and test. Lastly, new experiments to test other stressors, like temperature stress and hypoxic stress, may provide greater insight into the effect of nanoparticles. It is possible that nanoparticle-treated cells respond variably to different types of stress. Variation of results based on stress type can be helpful for narrowing the potential mechanisms responsible for cellular rescue.

CONCLUSION

In this study, we demonstrated the low serum starvation death of ARPE-19 cells to be curtailed when pretreated with cerium oxide nanoparticles. Cell viability was significantly higher when pretreating ARPE-19 cells with 500 µg/mL cerium oxide nanoparticles, as compared to the untreated control. These statistically significant differences could be seen in MTS assay when analyzing cells with low serum stress of 96 hours, specifically at 1% and 0.1% FBS concentrations.

With the results that we have presented, it is conceivable that nanoparticles can represent a novel treatment class to prevent progressive blindness in diseases such as age-related macular degeneration and photochemical damage from blue light.

Future experiments must be completed to test the effect of nanoparticles on ARPE-19 cells under other types of stress conditions, such as hypoxic stress or temperature stress. We have considered Bcl-2 protein inhibition as a possible mechanism of nanoparticle-induced cell rescue. Overall, more work must be completed to identify specific mechanisms behind nanoparticle-mediated rescue of ARPE-19 cells.

ACKNOWLEDGEMENTS

We would like to thank Northeastern University for funding this research and recognize Thomas Webster and Maximilian Bizanek for their contributions to these results. We would also like to acknowledge Dr. Demitrios Vavvas of Massachusetts Eye & Ear Infirmary for his consultation in the area of ophthalmology.

REFERENCES

- 1.Knickelbein JE, Chan CC, Sen HN, Ferris FL, Nussenblatt RB. Inflammatory Mechanisms of Age-related Macular Degeneration. *Int Ophthalmol Clin*. 2015; 55(3): 63-78.
- 2.Datta S, Cano M, Ebrahimi K, Wang L, Handa JT. The impact of oxidative stress and inflammation on RPE degeneration in non-neovascular AMD. *Prog Retin Eye Res*. 2017;

- 60:201-218.
- 3.Nita M, Strzałka-Mrozik B, Grzybowski A, Mazurek U, Romaniuk W. Age-related macular degeneration and changes in the extracellular matrix. *Med Sci Monit*. 2014; 20:1003- 1016.
- 4.Błasiak J, Piechota M, Pawłowska E, Szatkowska M, Sikora E, Kaarniranta K. Cellular Senescence in Age-Related Macular Degeneration: Can Autophagy and DNA Damage Response Play a Role?. *Oxid Med Cell Longev*. 2017; 2017: 5293258.
- 5.Bellezza I. Oxidative Stress in Age-Related Macular Degeneration: Nrf2 as Therapeutic Target. *Front Pharmacol*. 2018; 9: 1280.
- 6.Rohowetz LJ, Kraus JG, Koulen P. Reactive Oxygen Species-Mediated Damage of Retinal Neurons: Drug Development Targets for Therapies of Chronic Neurodegeneration of the Retina. *Int J Mol Sci*. 2018; 19(11): 3362.
- 7.Kunchithapautham K, Atkinson C, Rohrer B. Smoke exposure causes endoplasmic reticulum stress and lipid accumulation in retinal pigment epithelium through oxidative stress and complement activation. *J Biol Chem*. 2014; 289(21): 14534-14546.
- 8.Al-Zamil WM, Yassin SA. Recent developments in age-related macular degeneration: a review. *Clin Interv Aging*. 2017; 12: 1313-1330.
- 9.Kaliappan S, Jha P, Lyzogubov VV, Tytarenko RG, Bora NS, Bora PS. Alcohol and nicotine consumption exacerbates choroidal neovascularization by modulating the regulation of complement system. *FEBS Lett*. 2008; 582(23-24): 3451-3458.
- 10.Heesterbeek TJ, Lorés-Motta L, Hoyng CB, Lechanteur YTE, den Hollander AI. Risk factors for progression of age-related macular degeneration. *Ophthalmic Physiol Opt*. 2020; 40(2): 140-170.
- 11.Abokyi S, To CH, Lam TT, Tse DY. Central Role of Oxidative Stress in Age-Related Macular Degeneration: Evidence from a Review of the Molecular Mechanisms and Animal Models. *Oxid Med Cell Longev*. 2020; 2020: 7901270.
- 12.Galor A, Feuer W, Kempen JH, et al. Adverse effects of smoking on patients with ocular inflammation. *Br J Ophthalmol*. 2010; 94(7): 848-853.
- 13.Murat Dogru, Takashi Kojima, Cem Simsek, Kazuo Tsubota; Potential Role of Oxidative Stress in Ocular Surface Inflammation and Dry Eye Disease. *Invest. Ophthalmol. Vis. Sci*. 2018; 59(14): 163-168.
- 14.Golabchi K, Abtahi MA, Salehi A, Jahanbani-Ardakani H, Ghaffari S, Farajzadegan Z. The effects of smoking on corneal endothelial cells: a cross-sectional study on a population from Isfahan, Iran. *Cutan Ocul Toxicol*. 2018; 37(1): 9-14.
- 15.Kim GH, Kim HI, Paik SS, Jung SW, Kang S, Kim IB. Functional and morphological evaluation of blue light-emitting diode-induced retinal degeneration in mice. *Graefes Arch Clin Exp Ophthalmol*. 2016; 254(4): 705-716.
- 16.Zinlou C, Rochette PJ. Absorption of blue light by cigarette smoke components is highly toxic for retinal pigmented epithelial cells. *Arch Toxicol*. 2019; 93(2): 453-465.
- 17.Tosini G, Ferguson I, Tsubota K. Effects of blue light on the circadian system and eye physiology. *Mol Vis*. 2016; 22: 61-72.
- 18.Moon J, Yun J, Yoon YD, et al. Blue light effect on retinal pigment epithelial cells by display devices. *Integr Biol (Camb)*. 2017; 9(5): 436-443.

19. Dunn KC, Aotaki-Keen AE, Putkey FR, Hjelmeland LM. ARPE-19, a human retinal pigment epithelial cell line with differentiated properties. *Exp Eye Res.* 1996; 62(2): 155-169.
20. Yuan B, Webster TJ, Roy AK. Cytoprotective effects of cerium and selenium nanoparticles on heat-shocked human dermal fibroblasts: an in vitro evaluation. *Int J Nanomedicine.* 2016; 11: 1427-1433.
21. Singh R, Letai A, Sarosiek K. Regulation of apoptosis in health and disease: the balancing act of BCL-2 family proteins. *Nat Rev Mol Cell Biol.* 2019; 20(3): 175-193.